Revealing the Maximum Strength in Nanotwinned Copper

L. Lu, *et al.*

Science **323**, 607 (2009);
DOI: 10.1126/science.1167641

29. F. F. Balakirev *et al.*, *Phys. Rev. Lett.* **102**, 017004 (2009).
30. F. Rullier-Albenque *et al.*, *Phys. Rev. Lett.* **99**, 027003 (2007).
31. T. Senthil, *Phys. Rev. B* **78**, 035103 (2008).
32. A. Kanigel *et al.*, *Nat. Phys.* **2**, 447 (2006).
33. J. W. Loram, K. A. Mirza, J. R. Cooper, J. L. Tallon, *J. Phys. Chem. Solids* **59**, 2091 (1998).
34. T. Yoshida *et al.*, *J. Phys. Condens. Matter* **19**, 125209 (2007).
35. J. Zaanen, *Nature* **430**, 512 (2004).
36. J. W. Loram, J. Luo, J. R. Cooper, W. Y. Liang, J. L. Tallon, *J. Phys. Chem. Solids* **62**, 59 (2001).
37. C. Panagopoulos *et al.*, *Phys. Rev. B* **67**, 220502 (2003).
38. H. J. A. Molegraaf, C. Presura, D. van der Marel, P. H. Kes, M. Li, *Science* **295**, 2239 (2002).
39. S. Chakraborty, D. Galanakis, P. Phillips, http://arxiv.org/abs/0807.2854 (2008).
40. P. Phillips, C. Chamon, *Phys. Rev. Lett.* **95**, 107002 (2005).
41. We acknowledge technical and scientific assistance from S. L. Kearns, J. Levallois, and N. Mangkorntang and collaborative support from H. H. Wen. This work was supported by Engineering and Physical Sciences Research Council (UK), the Royal Society, *Laboratoire National des Champs Magnétiques Pulsés*, the French Agence Nationale de la Recherche IceNET, and EuroMagNET.

Supporting Online Material
www.sciencemag.org/cgi/content/full/1165015/DC1
Materials and Methods
Figs. S1 and S2
References

22 August 2008; accepted 21 November 2008
Published online 11 December 2008;
10.1126/science.1165015
Include this information when citing this paper.

Revealing the Maximum Strength in Nanotwinned Copper

L. Lu,[1]* X. Chen,[1] X. Huang,[2] K. Lu[1]

The strength of polycrystalline materials increases with decreasing grain size. Below a critical size, smaller grains might lead to softening, as suggested by atomistic simulations. The strongest size should arise at a transition in deformation mechanism from lattice dislocation activities to grain boundary–related processes. We investigated the maximum strength of nanotwinned copper samples with different twin thicknesses. We found that the strength increases with decreasing twin thickness, reaching a maximum at 15 nanometers, followed by a softening at smaller values that is accompanied by enhanced strain hardening and tensile ductility. The strongest twin thickness originates from a transition in the yielding mechanism from the slip transfer across twin boundaries to the activity of preexisting easy dislocation sources.

The strength of polycrystalline materials increases with decreasing grain size, as described by the well-known Hall-Petch relation (*1*, *2*). The strengthening originates from the fact that grain boundaries block the lattice dislocation motion, thereby making plastic deformation more difficult at smaller grain sizes. However, below a certain critical size, the dominating deformation mechanism may change from lattice dislocation activities to other mechanisms such as grain boundary–related processes, and softening behavior (rather than strengthening) is expected (*3*, *4*). Such a softening phenomenon has been demonstrated by atomistic simulations, and a critical grain size of maximum strength has been predicted (*5*–*7*). In pure metals, an impediment to determining the grain size that yields the highest strength is the practical difficulty of obtaining stable nanostructures with extremely small structural domains (on the order of several nanometers). The driving force for growth of nanosized grains in pure metals, originating from the high excess energy of numerous grain boundaries, becomes so large that grain growth may take place easily even at ambient temperature or below.

Coherent twin boundaries (TBs), which are defined in a face-centered cubic structure as the (111) mirror planes at which the normal stacking sequence of (111) planes is reversed, are known to be as effective as conventional grain boundaries in strengthening materials. Strengthening has been obtained in Cu when high densities of nanometer-thick twins are introduced into submicrometer-sized grains (*8*–*10*). In addition, coherent TBs are much more stable against migration (a fundamental process of coarsening) than conventional grain boundaries, as the excess energy of coherent TBs is one order of magnitude lower than that of grain boundaries. Hence, nanotwinned structures are energetically more stable than nanograined counterparts with the same chemical composition. The stable nanotwinned structure may provide samples for exploring the softening behavior with very small domain sizes. Here, we prepared nanotwinned pure Cu (nt-Cu) samples with average twin thickness ranging from a few nanometers to about 100 nm.

High-purity (99.995%) Cu foil samples composed of nanoscale twin lamellae embedded in submicrometer-sized grains were synthesized by means of pulsed electrodeposition. By increasing the deposition rate to 10 nm/s, we succeeded in refining the mean twin thickness (i.e., the mean spacing between adjacent TBs, hereafter referred to as λ) from a range of 15 to 100 nm down to a range of 4 to 10 nm (see supporting online material). The as-deposited Cu foils have an in-plane dimension of 20 mm by 10 mm and a thickness of 30 μm with a uniform microstructure. Shown in Fig. 1, A to C, are transmission electron microscopy (TEM) plane-view images of three as-deposited samples with λ values of 96 nm, 15 nm, and 4 nm, respectively. The TEM images indicate that some grains are irregular in shape, but low-magnification scanning electronic microscopy images, both cross section and plane view, show that the grains are roughly equiaxed in three dimensions. Grain size measurements showed a similar distribution and a similar average diameter of about 400 to 600 nm for all nt-Cu samples. Twins were formed in all grains (see the electron diffraction pattern in Fig. 1D), and observations of twins in a large number of individual grains revealed no obvious change in the twin density from grain to grain. Note that in all samples, the edge-on twins that formed in different grains are aligned randomly around the foil normal (growth) direction (*8*, *11*), in agreement with a strong [110] texture determined by x-ray diffraction (XRD). For each sample, twin thicknesses were measured from a large number of grains, which were detected from numerous TEM and high-resolution TEM (HRTEM) images, to generate a distribution. Figure 1E illustrates the 492 measurements for the sample with the finest twins; the majority yielded spacings between twins smaller than 10 nm, with a mean of 4 nm. For simplicity, each nt-Cu sample is identified by its mean twin thickness; for example, the sample with λ = 4 nm is referred to as nt-4.

Figure 2 shows the uniaxial tensile true stress–true strain curves for nt-Cu samples of various λ values. Also included are two stress-strain curves obtained from a coarse-grained Cu (cg-Cu) and an ultrafine-grained Cu (ufg-Cu) that has a similar grain size to that of nt-Cu samples but is free of twins within grains. Two distinct features are observed with respect to the λ dependence of the mechanical behavior of nt-Cu. The first is the occurrence of the λ giving the highest strength. All stress-strain curves of nt-Cu samples in Fig. 2, A and B, are above that of the ufg-Cu, indicating a strengthening by introducing twins into the submicrometer grains. However, such a strengthening does not show a linear relationship with λ. For λ > 15 nm (Fig. 2A), the stress-strain curves shift upward with decreasing λ, similar to the strengthening behavior reported previously in the nt-Cu (*9*, *11*) and nanocrystalline Cu (nc-Cu) (*12*–*15*) samples (Fig. 3A). However, with further de-

[1]Shenyang National Laboratory for Materials Science, Institute of Metal Research, Chinese Academy of Sciences, Shenyang 110016, P.R. China. [2]Center for Fundamental Research: Metal Structures in Four Dimensions, Materials Research Department, Risø National Laboratory for Sustainable Energy, Technical University of Denmark, DK-4000 Roskilde, Denmark.

*To whom correspondence should be addressed. E-mail: llu@imr.ac.cn

creases of λ down to extreme dimensions (i.e., less than 10 nm), the stress-strain curves shift downward (Fig. 2B). As plotted in Fig. 3A, the measured yield strength σ_y (at 0.2% offset) shows a maximum value of 900 MPa at $\lambda \approx 15$ nm.

The second feature is a substantial increase in tensile ductility and strain hardening when $\lambda < 15$ nm. As seen in Fig. 2, the tensile elongation of the nt-Cu samples increases monotonically with decreasing λ. When $\lambda < 15$ nm, the uniform tensile elongation exceeds that of the ufg-Cu sample, reaching a maximum value of 30% at the finest twin thickness. Strain-hardening coefficient (n) values were determined for each sample by fitting the uniform plastic deformation region to $\sigma = K_1 + K_2\varepsilon^n$, where K_1 represents the initial yield stress and K_2 is the strengthening coefficient (i.e., the strength increment due to strain hardening at strain $\varepsilon = 1$) (*16*, *17*). The n values determined for all the nt-Cu samples increase monotonically with decreasing λ (Fig. 3B), similar to the trend of uniform elongation versus λ. When $\lambda < 15$ nm, n exceeds the value for cg-Cu (0.35) (*16*, *17*) and finally reaches a maximum of 0.66 at $\lambda = 4$ nm. The twin refinement–induced increase in n is opposite to the general observation in ultrafine-grained and nanocrystalline materials, where n continuously decreases with decreasing grain size (Fig. 3B).

The strength of the nt-Cu samples has been considered to be controlled predominantly by the nanoscale twins via the mechanism of slip transfer across the TBs (*10*, *18*), and it increases with decreasing λ in a Hall-Petch–type relationship (*9*) similar to that of grain boundary strengthening in nanocrystalline metals (*12*). Our results show that such a relationship breaks down when $\lambda < 15$ nm, although other structural parameters such as grain size and texture are unchanged. The grain sizes of the nt-Cu samples are in the submicrometer regime, which is too large for grain boundary sliding to occur at room temperature, as expected for nanocrystalline materials with grain sizes below 20 nm (*3*). Therefore, the observed softening cannot be explained by the initiation of grain boundary–mediated mechanisms such as grain boundary sliding and grain rotation, as proposed by molecular dynamics (MD) simulations for nanocrystalline materials (*3*).

To explore the origin of the twin thickness giving the highest strength, we carried out detailed structural characterization of the as-deposited samples. HRTEM observations showed that in each sample TBs are coherent Σ3 interfaces associated with the presence of Shockley partial dislocations (as steps), as indicated in Fig. 1D. These partial dislocations have their Burgers vector parallel to the twin plane and are an intrinsic structural feature of twin growth during electrodeposition. The distribution of the preexisting partial dislocations is inhomogeneous, but their density per unit area of TBs is found to be rather constant among samples with different twin densities. This suggests that the deposition parameters and the twin refinement have a negligible effect on the nature of TBs. Therefore, as a consequence of decreasing λ, the density of such TB-associated partial dislocations per unit volume increases.

We also noticed that grain boundaries in the nt-Cu samples with $\lambda \leq 15$ nm are characterized by straight segments (facets) that are often

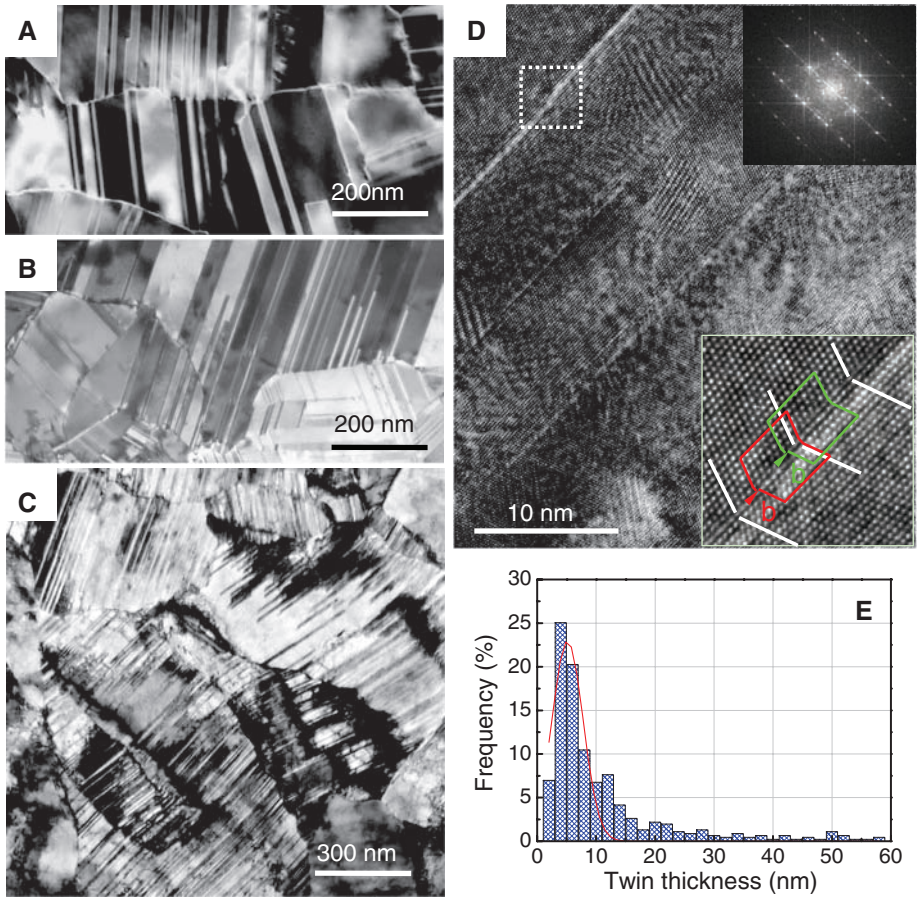

Fig. 1. TEM images of as-deposited Cu samples with various mean twin thicknesses. (**A**) $\lambda = 96$ nm. (**B**) $\lambda = 15$ nm. (**C**) $\lambda = 4$ nm. (**D**) The same sample as (C) but at higher resolution, with a corresponding electron diffraction pattern (upper right inset) and a HRTEM image of the outlined area showing the presence of Shockley partials at the TB (lower right inset). (**E**) Distribution of the lamellar twin thicknesses determined from TEM and HRTEM images for $\lambda = 4$ nm.

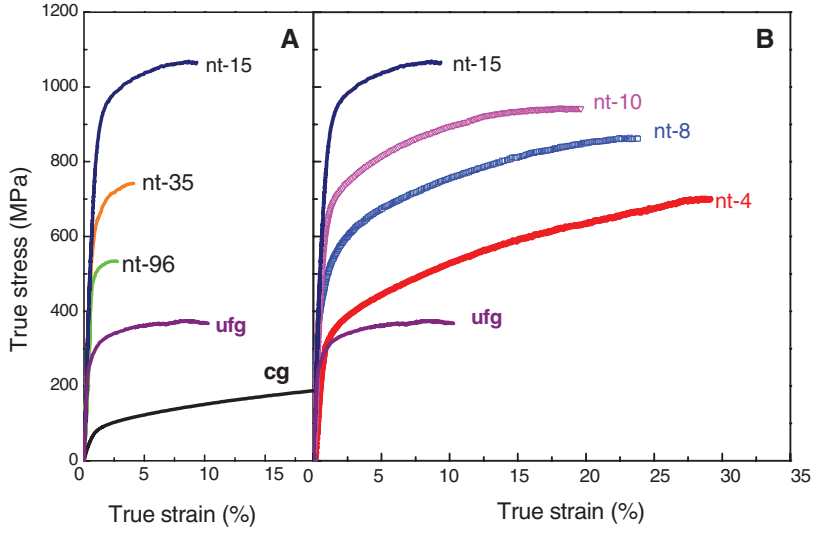

Fig. 2. Uniaxial tensile true stress–true strain curves for nt-Cu samples tested at a strain rate of 6×10^{-3} s^{-1}. (**A**) Curves for samples with mean twin thickness varying from 15 to 96 nm; (**B**) curves for samples with mean twin thickness varying from 4 to 15 nm. For comparison, curves for a twin-free ufg-Cu with a mean grain size of 500 nm and for a cg-Cu with a mean grain size of 10 μm are included.

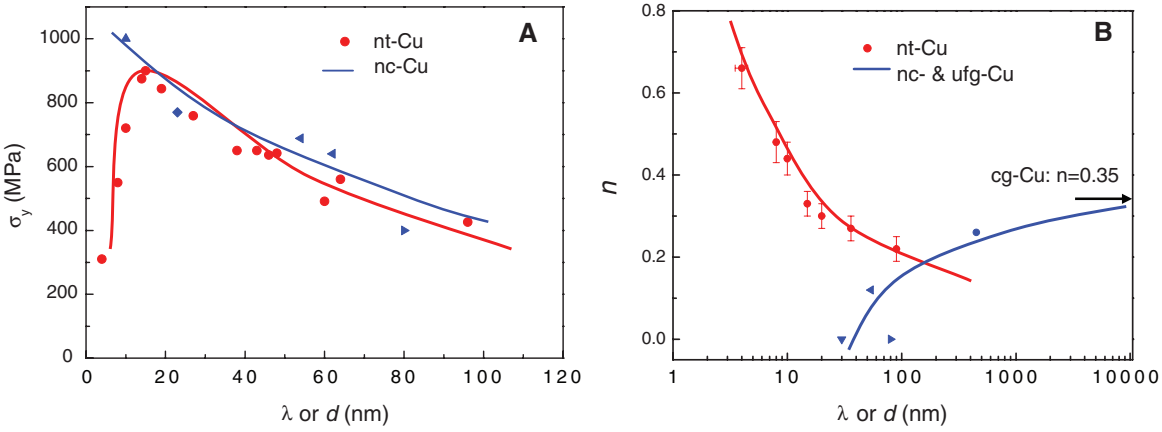

Fig. 3. Variation of (**A**) yield strength and (**B**) strain hardening coefficient n as a function of mean twin thickness for the nt-Cu samples. For comparison, the yield strength and n values for nc-Cu [▲ (*12*), ◀ (*13*), ▶ (*14*), and ◆ (*15*)], ufg-Cu [▼ (*9*)], and cg-Cu samples reported in the literature are included. A maximum in the yield stress is seen for the nt-Cu with $\lambda = 15$ nm, but this has not been observed for the nc-Cu, even when the grain size is as small as 10 nm.

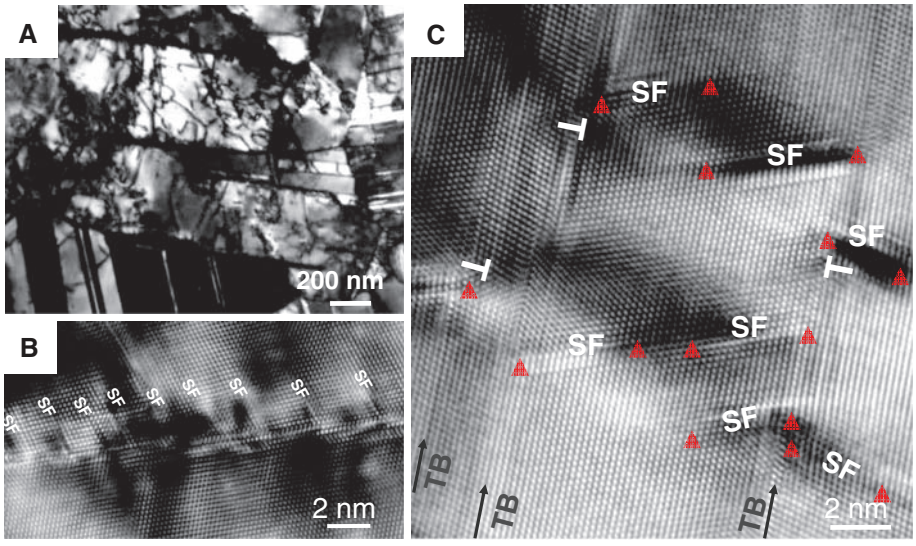

Fig. 4. (**A**) A typical bright TEM image of the deformed nt-96 sample showing the tangling of lattice dislocations. (**B**) An HRTEM image of the nt-4 sample tensile-deformed to a plastic strain of 30%, showing a high density of stacking faults (SF) at the TB. (**C**) The arrangement of Shockley partials and stacking faults at TBs within the lamellae in the nt-4 sample. Triangles, Shockley partial dislocations associated with stacking faults; ⊥, partials with their Burgers vector parallel to the TB plane.

associated with dislocation arrays (*19*), whereas in samples with coarser twins, grain boundaries are smoothly curved, similar to conventional grain boundaries. The microstrain measured by XRD was a negligible 0.01% for samples with $\lambda \geq$ 15 nm, but increased gradually from 0.038% to 0.057% when λ decreased from 10 to 4 nm, which also indicates a gradual increase in the defect density.

Recent experimental studies and MD simulations (*3*, *20*, *21*) have shown that an increase in the density of preexisting dislocations in nanoscale materials will cause softening. In the nt-Cu samples studied, both the dislocation arrays associated with the grain boundaries and the steps associated with the preexisting partial dislocations along TBs could be potential dislocation sources, which are expected to affect the initiation of plastic deformation (*22*) and to provide the dislocations required for the dislocation-TB interactions that cause work hardening. The preexisting partial dislocations can act as readily mobile dislocations, and their motion may contribute to the plastic yielding when an external stress is applied to the sample. The plastic strains induced by the motion of preexisting partial dislocations can be estimated as $\varepsilon = \rho_0 b_s d/M$ (where ρ_0 is the initial dislocation density, b_s is the Burgers vector of Shockley partial dislocation, d is the grain size, and M is the Taylor factor). Calculations showed that for the samples with $\lambda > 15$ nm, the preexisting dislocations induce a negligibly small plastic strain (<0.05%). However, for the nt-4 specimen, a remarkable amount of plastic strain, as high as 0.1 to 0.2%, can be induced just by the motions of high-density preexisting dislocations at TBs (roughly 10^{14} m^{-2}), which could control the macroscopic yielding of the sample. The above analysis suggests that for extremely small values of λ, a transition in the yielding mechanism can result in an unusual softening phenomenon in which the preexisting easy dislocation sources at TBs and grain boundaries dominate the plastic deformation instead of the slip transfer across TBs.

Shockley partial dislocations are always involved in growth of twins during crystal growth, thermal annealing, or plastic deformation. Shockley partials might be left at TBs when the twin growth is interrupted. Therefore, the presence of Shockley partials at some TBs is a natural phenomenon. Although these preexisting dislocations may have a small effect on the mechanical behavior of the samples with thick twins, the effect will be much more pronounced in the samples with nanoscale twins and/or with high preexisting TB dislocation densities such as those seen in deformation twins (*23*).

To understand the extraordinary strain hardening, we analyzed the deformation structures of the tensile-deformed samples. In samples with coarse twins, tangles and networks of perfect dislocations were observed within the lattice between the TBs (Fig. 4A), and the dislocation density was estimated to be on the order of 10^{14} to 10^{15} m^{-2}. In contrast, high densities of stacking faults and Shockley partials associated with the TBs were found to characterize the deformed structure of the nt-4 sample (Fig. 4, B and C), indicating the interactions between dislocations and TBs. Recent MD simulations (*18*, *24*, *25*) showed that when an extended dislocation (two Shockley partials connected by a stacking fault ribbon) is forced by an external stress into a coherent TB, it recombines or constricts into a perfect dislocation configuration at the coherent TB and then slips through the boundary by splitting into three Shockley partials. Two of them glide in the slip plane of the adjacent twin lamella, constituting a new extended dislocation, whereas the third one, a twinning partial, glides along the TB and forms a step. It is expected that with increasing strain, such an interaction process will generate a high density of partial dislocations (steps) along TBs and stacking faults that align with the slip planes in the twin lamellae, which may (or may not) connect to the TBs. Such a configuration of defects was observed, as shown in Fig. 4C. The density of partial dislocations in the deformed nt-4 sample

was estimated to be 5×10^{16} m^{-2} on the basis of the spacing between the neighboring partials and λ. This is two orders of magnitude higher than that of the preexisting dislocations and the lattice dislocations stored in the coarse twins. Such a finding suggests that decreasing the twin thickness facilitates the dislocation-TB interactions and affords more room for storage of dislocations, which sustain more pronounced strain hardening in the nt-Cu (*26*, *27*).

These observations suggest that the strain-hardening behavior of nt-Cu samples is governed by two competing processes: dislocation-dislocation interaction hardening in coarse twins, and dislocation-TB interaction hardening in fine twins. With a refining of λ, the contribution from the latter mechanism increases and eventually dominates the strain hardening, as revealed by the continuous increase of *n* values (Fig. 3B). However, the former hardening mechanism usually leads to an inverse trend, diminishing with size refinement (*17*).

Twins are not uncommon in nature, and they appear in various metals and alloys with different crystallographic structures. Extremely thin twin lamellae structures can possibly be achieved under proper conditions during crystal growth, plastic deformation, phase transformations, or thermal annealing of deformed structures. Our finding of the twin thickness giving maximum strength illustrates that the scale-dependent nature of plastic deformation of nanometer-scale materials is not necessarily related to grain boundary–mediated processes. This finding also provides insight into the development of advanced nanostructured materials.

References and Notes

1. E. O. Hall, *Proc. Phys. Soc. London Ser. B* **64**, 747 (1951).
2. N. J. Petch, *J. Iron Steel Inst.* **174**, 25 (1953).
3. J. Schiøtz, K. W. Jacobsen, *Science* **301**, 1357 (2003).
4. S. Yip, *Nature* **391**, 532 (1998).
5. M. A. Meyers, A. Mishra, D. J. Benson, *Prog. Mater. Sci.* **51**, 427 (2006).
6. P. G. Sanders, J. A. Eastman, J. R. Weertman, *Acta Mater.* **45**, 4019 (1997).
7. C. C. Koch, K. M. Youssef, R. O. Scattergood, K. L. Murty, *Adv. Eng. Mater.* **7**, 787 (2005).
8. L. Lu *et al.*, *Acta Mater.* **53**, 2169 (2005).
9. Y. F. Shen, L. Lu, Q. H. Lu, Z. H. Jin, K. Lu, *Scr. Mater.* **52**, 989 (2005).
10. X. Zhang *et al.*, *Acta Mater.* **52**, 995 (2004).
11. L. Lu, Y. Shen, X. Chen, L. Qian, K. Lu, *Science* **304**, 422 (2004); published online 18 March 2004 (10.1126/science.1092905).
12. J. Chen, L. Lu, K. Lu, *Scr. Mater.* **54**, 1913 (2006).
13. S. Cheng *et al.*, *Acta Mater.* **53**, 1521 (2005).
14. Y. Champion *et al.*, *Science* **300**, 310 (2003).
15. Y. M. Wang *et al.*, *Scr. Mater.* **48**, 1851 (2003).
16. A. Misra, X. Zhang, D. Hammon, R. G. Hoagland, *Acta Mater.* **53**, 221 (2005).
17. M. A. Meyers, K. K. Chawla, in *Mechanical Behavior of Materials*, M. Horton, Ed. (Prentice Hall, Upper Saddle River, NJ, 1999), pp. 112–135.
18. Z. H. Jin *et al.*, *Scr. Mater.* **54**, 1163 (2006).
19. X. H. Chen, L. Lu, K. Lu, *J. Appl. Phys.* **102**, 083708 (2007).
20. X. Huang, N. Hansen, N. Tsuji, *Science* **312**, 249 (2006).
21. Z. W. Shan, R. K. Mishra, S. A. Syed Asif, O. L. Warren, A. M. Minor, *Nat. Mater.* **7**, 115 (2008).
22. K. Konopka, J. Mizera, J. W. Wyrzykowski, *J. Mater. Process. Technol.* **99**, 255 (2000).
23. Y. S. Li, N. R. Tao, K. Lu, *Acta Mater.* **56**, 230 (2008).
24. S. I. Rao, P. M. Hazzledine, *Philos. Mag. A* **80**, 2011 (2000).
25. Z. H. Jin *et al.*, *Acta Mater.* **56**, 1126 (2008).
26. M. Dao, L. Lu, Y. Shen, S. Suresh, *Acta Mater.* **54**, 5421 (2006).
27. T. Zhu, J. Li, A. Samanta, H. G. Kim, S. Suresh, *Proc. Natl. Acad. Sci. U.S.A.* **104**, 3031 (2007).

28. Supported by National Natural Science Foundation of China grants 50431010, 50621091, 50725103, and 50890171, Ministry of Science and Technology of China grant 2005CB623604, and the Danish National Research Foundation through the Center for Fundamental Research: Metal Structures in Four Dimensions (X.H.). We thank N. Hansen, Z. Jin, W. Pantleon, and B. Ralph for stimulating discussions, X. Si and H. Ma for sample preparation, S. Zheng for TEM observations, and Y. Shen for conducting some of the tensile tests.

Supporting Online Material

www.sciencemag.org/cgi/content/full/323/5914/607/DC1
Materials and Methods
Table S1
References

24 October 2008; accepted 30 December 2008
10.1126/science.1167641

Control of Graphene's Properties by Reversible Hydrogenation: Evidence for Graphane

D. C. Elias,[1]* R. R. Nair,[1]* T. M. G. Mohiuddin,[1] S. V. Morozov,[2] P. Blake,[3] M. P. Halsall,[1] A. C. Ferrari,[4] D. W. Boukhvalov,[5] M. I. Katsnelson,[5] A. K. Geim,[1,3] K. S. Novoselov[1]†

Although graphite is known as one of the most chemically inert materials, we have found that graphene, a single atomic plane of graphite, can react with atomic hydrogen, which transforms this highly conductive zero-overlap semimetal into an insulator. Transmission electron microscopy reveals that the obtained graphene derivative (graphane) is crystalline and retains the hexagonal lattice, but its period becomes markedly shorter than that of graphene. The reaction with hydrogen is reversible, so that the original metallic state, the lattice spacing, and even the quantum Hall effect can be restored by annealing. Our work illustrates the concept of graphene as a robust atomic-scale scaffold on the basis of which new two-dimensional crystals with designed electronic and other properties can be created by attaching other atoms and molecules.

Graphene, a flat monolayer of carbon atoms tightly packed into a honeycomb lattice, continues to attract immense interest, mostly because of its unusual electronic properties and effects that arise from its truly atomic thickness (*1*). Chemical modification of graphene has been less explored, even though research on carbon nanotubes suggests that graphene can be altered chemically without breaking its resilient C-C bonds. For example, graphene oxide is graphene densely covered with hydroxyl and other groups (*2*–*6*). Unfortunately, graphene oxide is strongly disordered, poorly conductive, and difficult to reduce to the original state (*6*). However, one can imagine atoms or molecules being attached to the atomic scaffold in a strictly periodic manner, which should result in a different electronic structure and, essentially, a different crystalline material. Particularly elegant is the idea of attaching atomic hydrogen to each site of the graphene lattice to create graphane (*7*), which changes the hybridization of carbon atoms from sp^2 into sp^3, thus removing the conducting π-bands and opening an energy gap (*7*, *8*).

Previously, absorption of hydrogen on graphitic surfaces was investigated mostly in conjunction with hydrogen storage, with the research focused on physisorbed molecular hydrogen (*9*–*11*). More recently, atomic hydrogen chemisorbed on carbon nanotubes has been studied theoretically (*12*) as well as by a variety of experimental techniques including infrared (*13*), ultraviolet (*14*, *15*), and x-ray (*16*) spectroscopy and scanning tunneling microscopy (*17*). We report the reversible hydrogenation of single-layer graphene and observed dramatic changes in its transport properties and in its electronic and atomic structure, as evidenced by Raman spectroscopy and transmission electron microscopy (TEM).

Graphene crystals were prepared by use of micromechanical cleavage (*18*) of graphite on top of an oxidized Si substrate (300 nm SiO_2) and then identified by their optical contrast (*1*, *18*) and distinctive Raman signatures (*19*). Three types of samples were used: large (>20 μm) crystals for Raman studies, the standard Hall bar devices 1 μm in width (*18*), and free-standing membranes (*20*, *21*) for TEM. For details of sample fabrication, we refer to earlier work (*18*, *20*, *21*).

[1]School of Physics and Astronomy, University of Manchester, M13 9PL, Manchester, UK. [2]Institute for Microelectronics Technology, 142432 Chernogolovka, Russia. [3]Manchester Centre for Mesoscience and Nanotechnology, University of Manchester, M13 9PL, Manchester, UK. [4]Department of Engineering, Cambridge University, 9 JJ Thomson Avenue, Cambridge CB3 OFA, UK. [5]Institute for Molecules and Materials, Radboud University Nijmegen, 6525 ED Nijmegen, Netherlands.

*These authors contributed equally to this work.
†To whom correspondence should be addressed. E-mail: Kostya@manchester.ac.uk